

Near-perfect Collimation of Wide-Field Cassegrain Telescopes

DANIEL R. BLANCO

National Optical Astronomy Observatories, 950 North Cherry Avenue, Tucson, AZ 85719

Received 2011 June 12; accepted 2011 November 22; published 2012 January 9

ABSTRACT. I describe a simple new method for collimating a Cassegrain telescope that gives near-perfect correction over a wide field of view. This method was used to collimate the 6.5 m MMT in 2002 with remarkably good results. The first step is to point the primary mirror accurately at an object. When the M1 optical axis points exactly toward an object, it cannot contribute pointing error, coma, or anamorphic aberration to the image field. If these are present, they must come from M2. Adjusting M2 to correct both pointing error and coma yields perfect collimation, canceling off-axis anamorphic aberrations. I present an analytical basis for this method and compare it with methods that measure off-axis image aberrations directly. In most cases, the technique described here gives better results. I describe the collimation procedure we used at MMT and suggest an easier way to adapt this method to other telescopes.

1. INTRODUCTION

As a new generation of telescopes pushes to very wide image fields of more than 3° angular diameter, accurate collimation becomes crucial for obtaining the best performance. A common method for collimating a Cassegrain telescope makes use of a fiducial mark at the vertex of the secondary mirror. Surveying techniques are used to position the mirror by centering the fiducial mark onto the telescope mechanical axis with the mirror surface normal to it. The telescope is pointed to acquire an object, and the primary mirror is tilted to eliminate coma in the on-axis image as measured with a wavefront sensor. The next step is to point the telescope at several objects to build a pointing model based on elevation angle (or right ascension and declination for equatorial telescopes) that corrects the telescope pointing, compensating for several error sources that affect pointing, including miscollimation of the optics due to tube flexure. This yields accurate pointing, but if any tube flexure is present, the images will generally grow comatic as the telescope changes elevation.

The next stage in refining the performance uses the on-axis wavefront sensor to map image aberrations as a function of elevation angle. Most recent large telescopes are equipped with actively controlled primary-mirror supports and articulated optics, often by mounting the secondary mirror on a hexapod positioner. Coma is corrected by tilting the secondary mirror, while astigmatism, trefoil, and a few higher-order aberrations are corrected by adjusting the active-mirror supports.

Barring any major problems in the optics or mirror supports, this or some analogous technique produces excellent images on-axis and usually gives acceptable images over a modest field of view, but it is not sufficient to obtain perfect collimation. If there is any tube flexure, or some other mistake in the procedure, the

images obtained over wide fields will exhibit a distinctive, bilaterally symmetric, binodal pattern of astigmatism that changes with elevation angle. Several recent articles (McLeod 1996; Noethe & Guisard 2000; DiVittorio 2006; Thompson et al. 2007; Rakich et al. 2008; Morgan & Kaiser 2008) describe how to improve the collimation by sampling the off-axis image aberrations. These data can be analyzed to reconstruct the alignment of the telescope optics using a technique called image field tomography.

What has not been fully appreciated is the magnitude of the pointing error associated with a miscollimated condition. Of the six articles cited previously, only one mentions pointing error, even though it is quite large for any measurable anamorphic image aberrations. In practice, pointing error can provide a much stronger signal than direct measurement of the off-axis image aberrations, especially in the presence of seeing, tracking jitter, and other noise. Moreover, while the off-axis aberrations must be sampled at several points in the image field, pointing error can be determined from a single measurement.

This article describes a new method of collimation that was developed and implemented at the 6.5 m MMT during the winter of 2002, just before commissioning the $f/5$ secondary mirror, wide-field corrector, 1° multiobject spectrograph Hectospec, and the half-degree imager MegaCam. It is a simple, low-cost extension of surveying technique. After collimating using this technique, wavefront measurements taken over the full 1° field and out-of-focus images from the half-degree MegaCam imager confirmed the excellence of the image quality over the full field (Fabricant 2004).

For the widest fields, and for three-mirror telescopes now under construction, image field tomography is the widely favored approach. But in most cases, a comparison favors the method described here. The next section develops a basis for

comparing these two quite-different approaches. Sections 3 and 4 describe the procedure and discuss its limitations. Section 5 suggests a way to adapt this method to other telescopes.

2. BASIS

In a miscollimated telescope that is free of coma, the axis of the primary mirror points away from the object imaged at the center of the Cassegrain image field by an angle ψ . Schroeder (2000) gives expressions relating the pointing error due to secondary tilt and decenter, for the relation between tilt and decenter for a coma-free image field, and for the angular astigmatism (AAS) in a miscollimated telescope. With appropriate substitutions, Schroeder’s equation can be recast in terms of pointing error ψ for both classical Cassegrain (cc) and Ritchey-Chrétien (rc) telescopes:

$$\begin{aligned} \text{AAS}_{\text{cc}} &= \frac{\theta^2}{2 \cdot F} \cdot \left[\frac{M^2 + \beta}{M \cdot (1 + \beta)} \right] - \frac{\psi \cdot \theta}{2 \cdot F} \cdot \frac{M^2 - 1}{1 + \beta} \\ \text{AAS}_{\text{rc}} &= \frac{\theta^2}{2 \cdot F} \cdot \left[\frac{2 \cdot M^2 + M + \beta}{2M \cdot (\beta + 1)} \right] - \frac{\psi \cdot \theta}{2 \cdot F} \cdot \frac{M^2 - 1}{1 + \beta}, \end{aligned} \tag{1}$$

where β is the back focal distance normalized by the primary focal length, F is the system focal ratio, M is the system magnification, and θ is the angular field radius (in radians). Note that this describes the angular astigmatism centered on the chief ray; however, the chief ray is displaced from the primary axis an angular distance ψ . For a detector that remains centered on the primary axis, the on-axis image will develop astigmatism that can be determined by evaluating equation (1) at field point $\theta = \psi$, while the maximum difference in measurable astigmatism over the entire image field can be determined by evaluating equation (1) at field points $\theta + \psi$ and $\theta - \psi$ and taking the difference. The ratio of maximum differential astigmatism to pointing error provides a measure of the sensitivity of the system to pointing error. To a close approximation, the ratio is given by

$$\begin{aligned} \frac{\text{AAS}_{\Delta\text{cc}}}{\psi} &= \frac{\theta}{F} \cdot \frac{2(M^2 + \beta)}{M \cdot (1 + \beta)} \\ \frac{\text{AAS}_{\Delta\text{rc}}}{\psi} &= \frac{\theta}{F} \cdot \frac{2 \cdot M^2 + M + \beta}{M \cdot (1 + \beta)}. \end{aligned} \tag{2}$$

Table 1 lists parameters and evaluates the AAS_{Δ}/ψ ratio for several telescopes, including the 4.2 m Discovery Channel Telescope (DCT) and the 2×8.4 m Large Binocular Telescope (LBT). It ranges from about 1/30 to 1/450, depending on the field size. In other words, the pointing error ψ is typically more than 30" for 1" of miscollimation astigmatism. Conversely, if the pointing error can be reduced to 1", the differential astigmatism can be reduced to less than 1/30" (in many cases, much less).

TABLE 1

PARAMETERS FOR SEVERAL TELESCOPES USED TO CALCULATE RATIO OF ASYMMETRIC ANGULAR ASTIGMATISM TO POINTING ERROR FROM EQ. (2)

	F	M	B	θ (arcmin)	AAS_{Δ}/ψ
VISTA	3.041	2.79	0.295	60	1/34
SDSS	5	2.22	0.304	60	1/67
MMT	5.147	4.117	0.228	30	1/78
WIYN	6.289	3.574	0.442	30	1/125
VLT	15	8.33	0.174	15	1/228
DCT	6.1	3.2	0.476	15	1/273
LBT	15	12.9	0.363	6	1/445

The basis of this collimation technique lies in recognizing that when the primary mirror accurately points toward an object, it cannot contribute pointing error, coma, or asymmetric astigmatism to the image field. If these are present, they must come from misalignment of the secondary mirror. There is one unique position for the secondary mirror that produces an image that is both free of coma and centered on the M1 axis. In this position the axes of the primary and secondary mirrors coincide and the collimation is perfect.

In fact, there are at least five characteristic effects that arise from a miscollimated condition. Besides pointing error, miscollimation generally results in nonradially symmetric coma, anamorphic astigmatism, differential focus (image field tilt), and anamorphic field distortion. Table 2 ranks these effects in order of signal strength. Actual relative strengths are telescope-specific, but typically differ by an order of magnitude each. In principle, we could measure any two effects to obtain enough information for perfect collimation, thereby reducing the others to zero. For instance, one could collimate based on measurements of focus or field distortion, but in most cases the signals are exceedingly weak and may be subject to flexure and other systematic effects. Coma is the most pernicious image aberration, so it is commonly corrected first by tilting either the primary or the secondary mirror.

McLeod’s (1996) method corrects for coma, then astigmatism based on at least four measurements (McLeod used eight, and others used more). Though he did not say so, McLeod assumed that the telescope was constantly repointed as if by an

TABLE 2

MISCOLLIMATION EFFECTS IN DESCENDING ORDER OF RELATIVE SIGNAL STRENGTH AND MINIMUM NUMBER OF SAMPLES NEEDED PER MEASUREMENT

Effect	Samples
Pointing error	1
Coma	1
Δ Focus	3
Δ Astigmatism	4
Δ Field distortion	5

automatic guider. In effect, he ignored miscollimation pointing error completely. Other authors have followed suit. The present method corrects the pointing error first, then coma. This requires only one sample per measurement and takes advantage of the two strongest signals. Consequently, it is both more efficient and intrinsically more accurate.

3. COLLIMATION PROCEDURE

Our goal for this procedure was to limit anamorphic aberrations to less than $0.1''$. For the MMT this implies a pointing accuracy better than $8''$ (from Table 1). There are several steps to the process, each of which can introduce error. We resolved to try for accuracies better than $1''$ for each step. The new MMT is a classical Cassegrain telescope (purely parabolic primary mirror), with three secondary mirrors: an $f/9$ secondary for the suite of legacy instruments from the original 6×1.8 m Multiple Mirror Telescope, an $f/15$ adaptive secondary, and the $f/5$ secondary. Each secondary is mounted on a hexapod positioner that is capable of moving in five degrees of freedom. Prime focus is accessible inside the secondary support hub, though it is not used for science observations.

In the months prior to the arrival of the wide-field optics, we reviewed the initial alignment of the MMT optics and repeated key measurements. Using dial indicators, we verified the centration of the primary mirror to within 0.1 mm (about $2.5''$ on the sky) by indicating on the inner edge of the Cassegrain hole with a dial indicator mounted on the instrument rotator. We also verified that the primary mirror remains fixed to the mirror cell over the full elevation range of the telescope. In the MMT the primary is actively supported using feedback from six linear transducers that define the mirror kinematically to its cell.

We rechecked the alignment of the $f/9$ secondary using the technique described in the Introduction. Oddly, the prior collimation done in 2000 required tilting the primary mirror in its cell; for the first 2 yr of operation the back plate of the plano-concave 6.5 m mirror was inclined $3'$ with respect to its cell. This led to a dispute with the optics shop that had not been resolved.

Identifying the mechanical axis of a large bearing is by no means easy or straightforward. The MMT instrument bearing, like several others I have seen, has an angular wobble that causes the axis to wander in a Lissajous pattern of a several-arcsecond radius (Fig. 1). This tilt has negligible effect on the image field, but it does pose a challenge for defining the bearing "axis." After mapping the wobble pattern—which is repeatable—we chose a rotator position close to the center of the pattern and defined this to be the mean mechanical axis of the telescope.

During daytime, with the telescope at zenith pointing, we projected this axis onto a prime focus camera with a Keuffel & Esser autocollimating alignment telescope mounted on the rotator axis (Fig. 2). This device can project an image of its reticle coaxial to its line of sight within $1''$. We recorded the location of the projected reticle on the prime focus camera by marking a

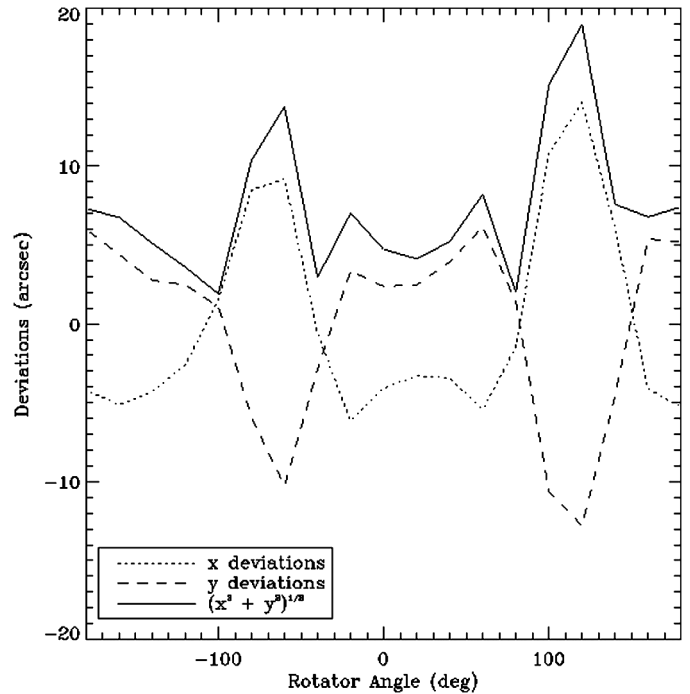


FIG. 1.—Angular wobble of the instrument rotator bearing. Though it affects alignment, the wobble has negligible impact on the performance of the telescope.

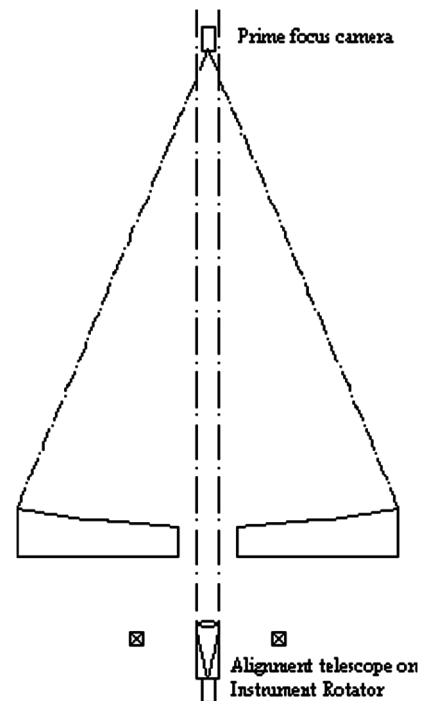


FIG. 2.—An alignment telescope on the instrument rotator was used to project the mean central axis of the bearing onto the prime focus camera.

video screen with a felt-tip marker—this was done very carefully, as it was our largest source of potential error.

That evening we acquired an object close to zenith using the prime focus video camera. The optical axis of a parabolic primary mirror can easily be found by examining the images at prime focus. There is a radially symmetric coma pattern that is quite strong for fast focal ratios (Fig. 3). When the primary mirror points directly toward an object, its image will be at the center of the prime focus coma pattern.

We found that the most effective way to locate the center of the coma pattern is to examine the out-of-focus images; these appear as donuts with a central obscuration produced by the Cassegrain hole and the secondary spider. When the primary is pointed directly toward an object, the central obscuration will be centered. But when the primary is pointed away from the object, the central obscuration will appear decentered due to coma (Fig. 4).

The angular length of the coma tail in the focused image is equal to the angular decentration of the central obscuration in the donut image, d_{co} . This can be determined by

$$d_{co} = \frac{3}{16} \cdot \frac{1 - \epsilon^2}{F_p^2} \cdot \psi, \quad (3)$$

where ϵ is the obscuration ratio (ratio of baffle to aperture diameter). F_p is the primary-mirror focal ratio, and ψ is the angular distance from the primary-mirror axis (pointing error).

This technique will be familiar to many amateur astronomers; it is similar to the method used for collimating a Newtonian telescope. It is quite accurate; we found that we could point the telescope repeatably to better than 1" when judging the centration of the donut by eye. This was more than sufficient to meet our goal for accuracy.

We tilted the primary mirror in its cell to move the center of the coma pattern onto the projected rotator axis. This should co-align the M1 optical axis to the telescope mechanical axis. We were pleased to find this procedure removed the 3' tilt introduced during the previous collimation 2 yr prior. This resolved the dispute with the optics shop and confirmed that the primary-mirror optical axis is precisely normal to its back plate.

We devised a rather ingenious means of verifying this alignment. The prime focus camera that we used is a compact cylindrical package about 25 mm diameter, smaller than the 50 mm beam of the K&E. When properly aligned we could simultaneously see images of the star in the prime focus camera, the star image in a second video camera mounted at the K&E eyepiece, and the reticle projected from the K&E onto the prime focus camera (refer to Fig. 2). In this way we confirmed the co-alignment of the optical and mechanical axes to within about an arcsecond. This was verified close to zenith pointing. Off-zenith, flexure in the K&E mount introduced a systematic effect that led us, at first, to suspect that M1 was sagging in its cell.

We built a pointing model by locating the center of the coma field at several elevation angles and determining the pointing offset needed to move the star image to the center of its coma field. This technique is insensitive to flexure of the top end; it is based on the center of the coma pattern, regardless of its position on the camera. A pointing model built from these measurements became the master pointing model for the telescope and has not changed since.

After installing the secondary mirror we pointed the telescope using the master M1 pointing model. The resulting image was decentered and comatic. We tilted the secondary about its coma-neutral point to move the image to the center of the instrument rotator, then tilted about its center of curvature to eliminate

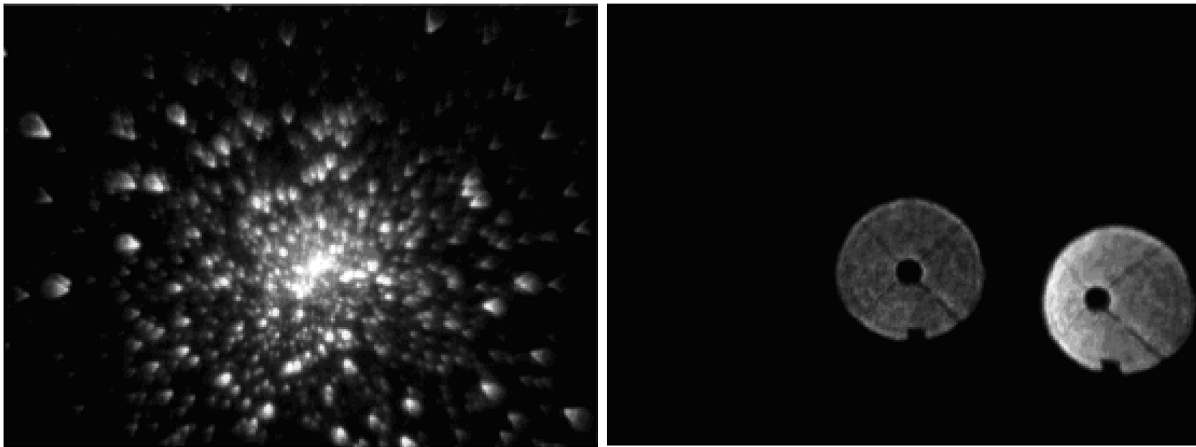


FIG. 3.—Two frames obtained at prime focus of the MMT. *Left*: A rich field; the coma tails point toward the optical axis of the primary. *Right*: A field with just two stars—here, the images are defocused to approximately 10" diameter. Comatic decentration of the central obscuration points toward the primary-mirror axis. The small square at the bottom of the two images is a flag used to map the image orientation.

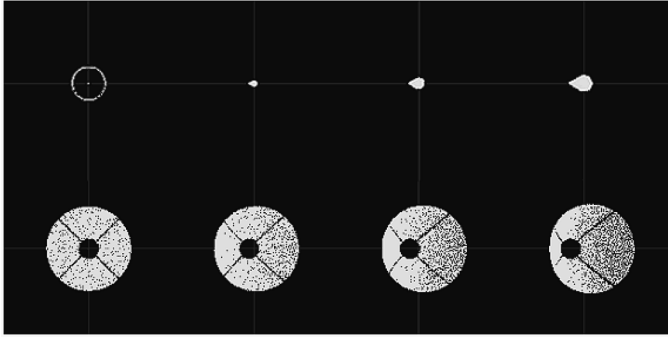


FIG. 4.—Simulated prime focus images for an $f/2$ parabolic mirror with a central obscuration. These images show the effect of coma for in-focus (*top*) and for images that are defocused to about $2.5''$ diameter (*bottom*). *Left*: On-axis. *Right*: 5, 10, and $15''$ off-axis. The circle at the upper left is $1''$ in diameter.

coma. We repeated this procedure at several elevation angles to build an elevation-dependent model for positioning the secondary-mirror hexapod. This took about 6 minutes at each elevation. This was repeated for all three secondary mirrors, always using the master pointing model; only the commands to the hexapods differ between configurations. Wavefront analysis and image metrology over the full 1° diameter field confirmed that this procedure gave accurate collimation that more than satisfied the $0.1''$ requirement.

In operation, secondary changes can be done with minimum effort; there is no need for precision alignment after a secondary change, nor is it necessary to examine off-axis images or analyze aberration patterns. After installing a new secondary mirror, we acquire a star using the master pointing model. Usually, the image is not centered in the field and is comatic. We tilt the secondary about its coma-neutral point to move the image onto the center of the image field, then tilt about its center of curvature to eliminate coma as measured with a wavefront sensor. Once the telescope is collimated any residual astigmatism in the on-axis image must be due to mechanical distortion in the optics; thus, the same on-axis measurement can be used to adjust the primary-mirror active supports. In practice, at the start of the night we repeat the initial on-axis wavefront analysis 3 times to be sure of convergence (Blanco 2004).

4. LIMITATIONS

As with any alignment procedure, this technique is limited by the precision obtained at each step:

1. Mechanically center the primary mirror.
2. Locate the axis of the instrument rotator.
3. Project the axis to prime focus.
4. Locate the optical axis of the primary.
5. Co-align the M1 optical and mechanical axes.
6. Build a pointing model true to the M1 optical axis.
7. Adjust M2 to eliminate coma and correct the pointing.

Equation (2) can be used to assess the residual astigmatic aberration due to errors in the procedure. For the MMT we estimate that we obtained an overall precision better than $3''$, sufficient to reduce the residual anamorphic astigmatism to less than $1/30''$ at the edge of the 1° field.

The secondary support structure or central baffle may not be perfectly centered on the mechanical axis of the telescope. Thus, there are two possible sources of apparent decentration: one due to coma and the second due to a mechanical error in the alignment of the baffle. Unlike decenter due to coma, a mechanical decenter will shift through focus—appearing on one side or the other above or below focus. The decenter due to coma is a much stronger effect; as long as the baffle is reasonably well aligned, the resulting error will be quite small. Moreover, it can be negated by repeating measurements on either side of focus.

As implemented at MMT, the technique depends on the use of elevation-dependent lookup tables. These in turn rely on the integrity of the telescope structure linking the primary mirror to the elevation encoder. Flexure and hysteresis along this path limit the repeatability of the M1 pointing model and, consequently, the accuracy of collimation. Fortunately, this load path is short and stiff in most modern altitude-azimuth telescopes. By far, the largest source of pointing error in most telescopes is flexure in the secondary-mirror support structure. Rather than re-point the entire telescope, as is commonly done, the way to maintain near-perfect collimation is to adjust the secondary mirror to center the image while simultaneously correcting coma.

5. ADAPTING THIS METHOD TO OTHER TELESCOPES

In its most general form, this method adds an external reference to the primary mirror so that it can be accurately pointed. At the MMT this took the form of a lookup table based on a one-time measurement of the prime focus image field, but it could have been done more easily by adding an auxiliary line-of-sight (LOS) telescope, rigidly attached to the primary mirror and accurately aligned to the M1 axis, rather like adding a sighting scope to a rifle.

The LOS telescope would be used intermittently to reset telescope pointing at the start of each night and periodically to update the master M1 pointing model. In principle, it can be used exactly like an automatic guider, providing a continuous signal for tracking the telescope. Any of several methods can be used to align the LOS telescope to the M1 axis: a one-time measurement of the off-axis image aberrations, for example. Once the external reference is in place and aligned, a single wavefront sensor measuring wavefront tilt and coma at the combined focus is all that is needed to obtain near-perfect collimation. It is convenient to make this measurement on axis, but it could be done anywhere in the field. This arrangement should be able to maintain near-perfect collimation indefinitely at low initial cost and minimal operational overhead.

The basic technique can be extended to three-mirror telescopes by fitting both M1 and M2 with auxiliary LOS telescopes. The Large Synoptic Survey Telescope (LSST), currently in construction, would only need one, since the primary and tertiary mirrors are polished into a single monolithic substrate.

6. SUMMARY AND CONCLUSION

There is a basic uncertainty when the two mirrors of a Cassegrain telescope are initially assembled and collimated; there are infinite combinations of tilts and decenters for M1 and M2 that produce excellent images on axis, but only one that gives perfect collimation over a wide field. The effect of miscollimation is noticeable in the off-axis images, so intuition suggests that we can examine these to determine how to correct the collimation. This method works well; the Visible and Infrared Survey Telescope for Astronomy (VISTA) now operates in this way, and other wide-field projects plan to implement similar systems. But measuring the requisite number of images is a slow, tedious process when done manually, and it is expensive to automate.

This article describes an alternate approach based on measurement of pointing error that can be implemented at a small

fraction of the cost. It uses the strongest two signals that arise from miscollimation. In general, alignment that is based on stronger signals will have better accuracy and less noise than alignment based on any of the weaker signals. Pointing error provides a signal that is directly proportional to off-axis anamorphic aberration, but many times stronger. It can be measured by a device that is no more complicated or expensive than an automatic guider.

It is worth mentioning a corollary conclusion: telescopes that have multiple secondary mirrors, or prime, Cassegrain, and Nasmyth foci should have only one pointing model. For proper collimation the model must accurately point the primary mirror. As long as the telescope points true to the primary mirror, near-perfect collimation is a simple task.

I would like to thank Brian McLeod for his tireless help in implementing this technique at the MMT over many long cold nights during the winter of 2002. Particular thanks to Dan Schroeder for help with the math; to Lothar Noethe, Mike DiVittorio, Andrew Rakish, and Jeff Morgan for their helpful comments and corrections; and to my *PASP* referee for his insightful comments.

REFERENCES

- Blanco, D., et al. 2004, *Proc. SPIE*, 5489, 300
 DiVittorio, M. 2006, *Proc. SPIE*, 6273, 62733D, DOI: 10.1117/12.672856
 Fabricant, D., et al. 2004, *Proc. SPIE*, 5492, 767
 McLeod, B. A. 1996, *PASP*108217
 Morgan, J. S., & Kaiser, N. 2008, *Proc. SPIE*, 7012, 70121K, DOI: 10.1117/12.788426
 Noethe, L., & Guisard, S. 2000, *Proc. SPIE*, 4003, 382
 Rakich, A., et al. , *Proc. SPIE*, 7012, 70121L, DOI: 10.1117/12.789902
 Schroeder, D. J. 2000, *Astronomical Optics*, (2nd ed.; New York: Academic Press)
 Thompson, K., Schmid, T., & Roland, J. 2007, *Proc. SPIE*, 6834, 68340B, DOI: 10.1117/12.772010